

Ndumiso Mthembu¹, Hlamulo Ndlovu¹, Bright Ndebele¹, Kevin Jamison¹ & Lindokuhle Zwane¹

¹Aeronautic Systems Impact Area, Council for Scientific and Industrial Research (CSIR), Pretoria, South Africa

Abstract

A method optimised for efficient prediction of subsonic store separation trajectories is described and demonstrated using a wind-tunnel test case. The FastTraj method uses a decoupled flow field approach where it is assumed that in most attached flow subsonic store separation scenarios the presence of the store has little impact on the perturbed flow field generated by the parent aircraft. The inviscid perturbed flow field of the parent aircraft is computed using computational fluid dynamics codes and is captured using a grid. The store aerodynamic model is generated elsewhere and Missile Datcom is used to segment the store model to approximate the effect of the perturbed flow field changing along the length of the store. The 6-DOF trajectory solver interpolates the aerodynamic grid from the parent aircraft to determine the local flow vector at each reference point on the segmented store, in addition to the local flow vector due to the motion of each segment. Good comparisons with the wind-tunnel data are achieved showing that the method's speed is not at the expense of accuracy and that it is necessary to segment the store to achieve good results.

Keywords: store, separation, CFD, subsonic, decoupled.

Nomenclature

 C_A , C_Y , and C_N store axial, side and normal force coefficients, respectively

 $\mathcal{C}_l,\,\mathcal{C}_m,$ and \mathcal{C}_n store rolling, pitching and yawing moment coefficients, respectively

 α , AOA angle of attack β , AOS angle of sideslip

 M_{∞} freestream Mach number q_{∞} freestream dynamic pressure

Reynolds number

 ψ_{ac} , α_{ac} , and ϕ_{ac} yaw, pitch and roll angle, respectively

 I_{XX} , I_{YY} , and I_{ZZ} moment of inertia about the x, y and z axis, respectively

1. Introduction

1.1 Overview of store separation

When a store is integrated with an aircraft, many changes are introduced to the characteristics of the aircraft, affecting its airworthiness [1][2]. These changes include the aircraft's performance, handling qualities and structural dynamics, amongst others. It is important to assess the nature and extent of the changes incurred, to maintain crew and platform safety and to ensure mission success. Such assessments are costly and time-consuming [3].

The separation of the store from the aircraft is often a high-risk aspect of the integration exercise.

Store separation may be required as a part of the normal employment of the store, such as releasing a bomb over a target [4], or it may be an emergency action in the event of a malfunction which requires the rapid but inert jettison of stores from the carrier aircraft in the interest of saving the aircraft. Store jettison may also be required to quickly improve the aircraft's performance and handling qualities such as when responding to threats [5]. The requirements and applications for store separation analysis are broad; thus, it is important to continue optimising the store separation analysis process.

The task of determining whether a store could be safely released has progressed from initially being performed by a "hit or miss" method where the store is released from the aircraft at incrementally higher speeds until the targeted release condition has been achieved or the release produces an unsafe scenario such as making contact with the carrier aircraft [2]. Contemporary methods are beneficiaries of the development of comprehensive guidelines and standards for certifying an aircraft-store configuration [5][6] and the use of assessment techniques such as experimental and computational simulations. These developments have significantly reduced the costs and enhanced the safety of conducting store separation tests.

When certifying a store for operational service on a particular aircraft, a full investigation of all the required aircraft-store configurations, deployment scenarios and emergency scenarios should be performed. This results in a large matrix of separation scenarios that must be assessed [7][7]. The scale of the task escalates when the guidance provided in MIL-HDBK-244A §5.1.1.2.3.1(g) [6][6][6] is considered. This document advises that variations in the aircraft release attitude, ejector impulse, and store mass and inertial properties, amongst others, should be analysed to show that they do not adversely affect the aircraft or the store during separation [6][6][6]. This large matrix of separation simulations can take a significant amount of time and resources to complete.

1.2 Methods for simulating store separation trajectories

The task of analysing separation scenarios has significantly improved the safety and cost of integrating stores. This initially began with experimental aerodynamic simulations in the form of wind tunnel tests and gradually progressed into the computational domain [2], with a combination of wind-tunnel and computational approaches being widely used [8]. Within each of these domains of simulation there are different ways of simulating store trajectories. Some methods are presented in Table 1.

	Wind tunnel simulation	Computational simulation
1	Captive trajectory simulation (CTS)	Time-accurate (full computation of flow field every step)
2	Free drop tests	Grid analysis (use grid with store present to characterise non-linear flow field computationally or in the wind-tunnel, which is then interpolated)
3	-	Decoupled flow field (the flow field is calculated or measured in the wind-tunnel without the store present)

Table 1 – Means of simulating the trajectory of a store released from an airborne aircraft.

The CTS method involves having an aircraft and store model mounted on separate supports, within a wind tunnel test section, and moving each relative to one another to simulate the release of the store. The separation simulation is conducted in a quasi-steady state fashion where the store loads are measured at a particular position/orientation and then the store moved to the next, by a six-degree-of-freedom (6-DOF) algorithm, based on those measured loads [3].

Free drop testing is conducted with the parent aircraft model supported in the tunnel (by a sting, for example) and the store is released freely from the parent model by a mechanism representing the separation means and allowed to travel unconstrained though the flow field generated by the parent model. This form of simulation may capture unsteady effects which are omitted in the CTS test but require compromises in the scaling laws and are challenging to implement productively [3]. If a small

number of separation scenarios are being investigated, CTS and free drop tests are viable, but it is a lengthy and costly process to prepare the store and parent wind-tunnel models, in addition to the effort required to perform the tests. CTS tests are often done to validate trajectories generated using grid data measured in wind-tunnels and/or CFD.

Time accurate simulations involve the solving of the flow conditions for each time step as the store traverses the flow field [9]. This can be implemented using Reynolds Averaged Navier-Stokes (RANS) or Euler CFD codes or with panel codes. Implementation with CFD requires the use of various methods to address the impact of the relative movement of the aircraft and store on the flow field mesh [10]. Implementation in panel codes requires the recalculation of the Aerodynamic Influence Coefficient (AIC) matrix for each time step [11]. Time accurate simulations are considered to be the most accurate computational approach as the mutual aircraft/store aerodynamic interference is calculated at each time step, but it is computationally expensive, and a considerable amount of run time is required [11]. The use of this method has grown dramatically with the substantial increases in CFD cluster computing power [12].

The grid analysis method involves the generation of a grid of store positions and orientations in the region that the store is expected to translate after release, from its pylon on the parent aircraft [13]. The store is placed at each grid point either in the wind-tunnel or using computational aerodynamics. relative to the parent aircraft, and its loads in the aircraft flow field are measured for a given parent aircraft flight condition (e.g. Mach number, angle of attack (AOA) and sideslip angle). These loads are used to populate a look-up table which is used in an offline computer program to determine the trajectory of the store based on its initial conditions and loads along the trajectory. The wind-tunnel test may use the same test apparatus as the CTS method, where both models are supported, but in this case the store is placed in discrete positions on a grid within the aircraft flow field for a given flight condition and aircraft attitude [3]. A wind tunnel balance within the sting supporting the store measures the aerodynamic loads on the store model. Alternatively, the loads are computed using CFD [14] or panel codes. The grid method is mostly used when there is significant mutual aerodynamic interference between the aircraft and the store, which is often the case in transonic and supersonic store releases [8]. The influence function method is commonly used with the grid method which allows the grid data to be used for separation analyses of stores that have similar geometries, resulting in significant cost savings [15].

van den Broek [11] showed that in many cases, the impact of the aircraft and store mutual aerodynamic interference on the predicted store trajectory is small and may be neglected. In this work, the non-uniform flow field was characterised by calculating the perturbation field caused by the aircraft and applying this to a uniform flow field grid encompassing the volume expected to be traversed by the store after release. The trajectory of the store is calculated by interpolating the grid data to the current store position to determine the local perturbed flow field. In van den Broek's implementation using the panel code USTORE, the paneled store uses the grid to determine the local flow field parameters at each panel on the store. This method enables the flight condition to be changed with minimal effort as the aircraft and store AIC matrices do not need to be recalculated and changes to the initial conditions of the store, its mass, or inertial properties can be analysed without recalculating the flow field. A similar approach to separately determining the aircraft perturbation flow field and then mathematically superimposing the store is used in the United States Air Force (USAF) FLIP 4 Store separation trajectory simulation code [16]. In this code the aerodynamic characterisation of the store can be done using the called Missile Distributed Airloads (MDA) code. MDA is a semi-empirical software program that employs the component build-up method to estimate the loads on a store at a given attitude and flight condition. This build-up method enables the code to determine force and moment coefficients for each component of the store and account for the change in these coefficients based on the variations in the local flow conditions when the store is in a non-uniform flow field [17]. The approach used by van den Broek and FLIP 4 will be referred to as the "decoupled flow field" method in this paper.

2. The fast decoupled store separation analysis method

This paper presents the extension of the decoupled flow field method to the use of inviscid aircraft flow fields computed by CFD codes and a segmented model of the store that captures flow field perturbations along the length of the store and aerodynamic damping in the trajectory. This method is applied to a subsonic store separation analysis test case. While decoupled flow field techniques are widely used, the combination of CFD computed inviscid flow fields and segmented store models is novel. The perturbed aircraft flow field is typically computed using RANS CFD. This paper will show that acceptable results are quickly obtained at much lower cost using inviscid CFD solutions.

The question arises: why are panel codes not used to compute the inviscid perturbed aircraft flow field as journal articles like van den Broek [11] demonstrated to be acceptable? While panel codes give good results in the hands of well-trained users, the setup time for new projects is significant. Modern CFD packages and grid generators are well integrated with computer-aided design (CAD) packages and with modern computational resources, inviscid CFD simulation projects can be executed more quickly than with panel codes. A key limitation of the decoupled flow field method is that it is not applicable to scenarios where there is significant mutual aerodynamic interference between the aircraft and the store. This applies to transonic flow fields where shockwaves are present between the aircraft and the store, and to subsonic conditions with large stores positioned very close to the aircraft (e.g. the large drop tanks on the Mirage 2000 positioned close to the wing is an example).

In this section, we describe the procedure and its implementation using CFD, an empirical missile aerodynamics code and a six-degree-of-freedom (6-DOF) solver. While it was implemented using a specific CFD code, missile aerodynamics code, and a 6-DOF solver (viz. Star-CCM+ [19], Missile Datcom [20] and ARUV), the method presented will work with other similar solvers. The use of Missile Datcom is not necessary provided that the aerodynamic properties of the store are known by other means.

This section is split into two; Sections 2.1 and 2.2, each describing the philosophy of the method and its implementation, respectively. The implementation of this method is demonstrated and verified using a subsonic wind-tunnel store separation test case published by Roberts and Myers [18].

2.1 Method Description

A key assumption made in this method is that the influence of the store on the subsonic flow field around the parent aircraft is negligible in the period immediately after the store is released. On this basis, the perturbed velocity flow field around the parent aircraft and excluding the store can be calculated and subsequently imposed on the store. The Star-CCM+ CFD solver is used in this paper. When the velocity flow field around the parent aircraft has been determined, the region where the store is expected to be during the separation is resampled onto a coarser grid than the mesh used in the CFD simulation. Figure 1 shows an example of such a sampling grid below a parent model. The sampling grid is created so that its coarseness increases monotonically with the vertical distance from the parent model. This accounts for the decreasing perturbation of the flow field with increasing distance from the aircraft. This resampled velocity field is then imposed onto the segmented store to determine the trajectory.

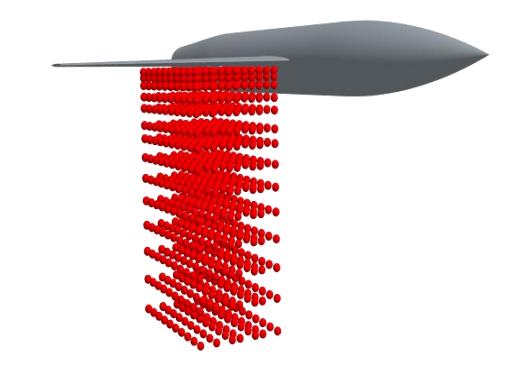


Figure 1 – A sampling grid below the starboard wing of the swept wing/fuselage model [18].

Figure 2 illustrates a store segmentation where the Roberts and Myers store has been split into the

nose cone, the centre body, and the aft body. The primary goal for the segmentation in this instance is to be able to capture localised effects that would not be possible if the store were treated as a rigid monolith. When the store has been segmented, the aerodynamic properties of each segment can be approximated using a tool such as Missile Datcom. When combined, the aerodynamic properties of the three store segments must add up to the aerodynamic properties of the complete store.

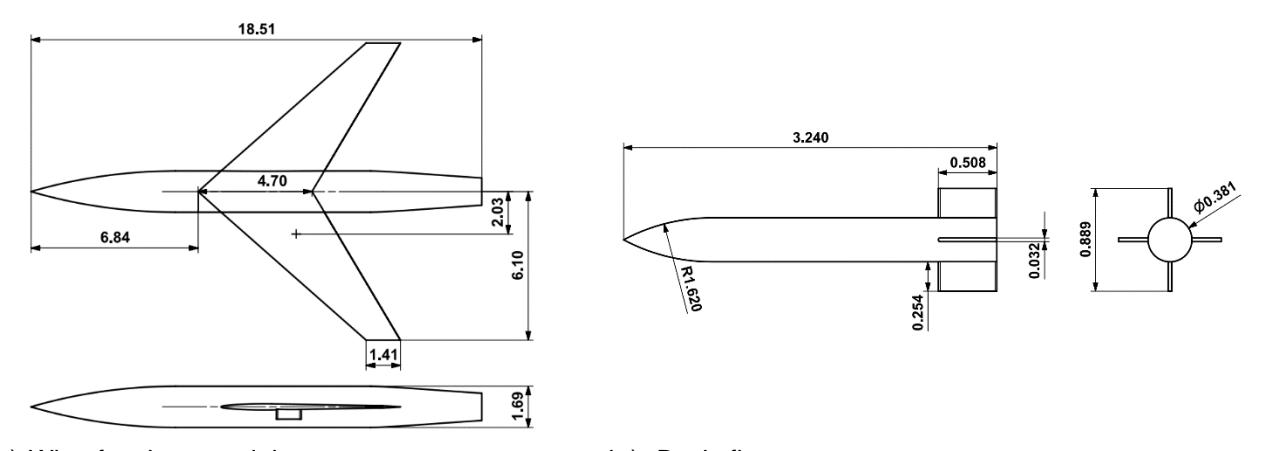


Figure 2 – An illustration of a store that has been segmented into three components.

With the aerodynamic properties of the store and the velocity flow field through which the store will move known, a 6-DOF solver can be used to calculate the trajectory and attitude of the store. This method is called FastTraj.

2.2 Implementation

The procedure described in Section 2.1 is demonstrated with the Roberts and Myers [18] models using Star-CCM+ to calculate the velocity flow field; Missile Datcom to determine store aerodynamic properties; and an inhouse 6-DOF solver called ARUV to calculate store trajectories upon store release.



a.) Wing fuselage model.

b.) Basic finner store.

Figure 3 – Sketches of the parent aircraft model (a) and store model (b) used to demonstrate the decoupled store trajectory method[18]. The dimensions are shown in meters.

Figure 3 shows the dimensions of the parent and store models. The calculation of the aerodynamic properties of the store in Figure 3b, the velocity flow fields, and finally the trajectories are described in the following sections.

2.2.1 Store Aerodynamics

Missile Datcom was used to estimate the aerodynamic properties of the store. Missile Datcom is a widely used semi-empirical software tool for the analysis of aerodynamic properties of axisymmetric missiles and aircraft [20]. The store loads are calculated from aerodynamic coefficients extracted from lookup tables that cover the incidence angle and Mach range expected from the store motion profile. The reference points for the segmented store were taken as follows, refer to Figure 4:

- The nose of the store is taken as the origin.
- The nose reference point is at one-third (1/3) of the nose length (LNOSE).
- The centre body reference point is at half (1/2) of the centre body length (LCENTRE) plus the nose length.
- The aft or tail body reference point is at half (½) of the tail length (LAFT) plus the nose and

centre body length.

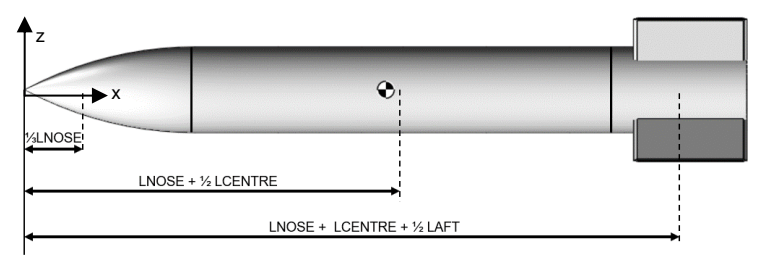


Figure 4 – Full store reference points

The store was segmented as illustrated in Table 2 and

Table 3. Segmentation allows for the respective aerodynamic contributions of the body segments to the overall store dynamics to be calculated and captures the store damping. The aerodynamic coefficients that were calculated for the overall store and for each segment were force coefficients such as C_X , C_Y , and C_Z and moment coefficients such as C_I , C_M , and C_R .

The aerodynamic coefficients for the sub-models were calculated using Missile Datcom by considering each segment as an individual body. By assuming linear superposition, the aerodynamic coefficients for the individual model segments were derived through appropriate subtraction of the sub-models, which were derived from Figure 4 and illustrated in Table 2 and Table 3. The 'X termination' distance is the axial coordinate at which the sub-models were terminated. The 'X reference' is the axial coordinate at which the local flow conditions are to be extracted and which then serves as a reference to find the appropriate matching data in the aerodynamic lookup tables. Table 2 also indicates sub-models which were ran to extract aerodynamic coefficients inside Missile Datcom.

The procedure followed in developing the model was to automate the process of loading store aerodynamic data, creating store segments, and writing the aerodynamic data into a segmented look-up table is shown in Figure 5. The first output file is a verification text file showing the verification of the store segment, at which it checks whether the three segments combined correctly adds up to the original store aeromodel (A + B + C = 1) at every Mach number, AOA and β combination. Other outputs include the segmented look-up table, non-segmented look up table (to compare segmented look-up table against non-segmented look-up table results) and plots to show individual contributions of the components to the overall aerodynamics of the store (see Figure 6, which shows the graph of C_m and the corresponding C_Z at $\beta = -21^\circ$ and Figure 7, which shows the C_n graph and the corresponding C_Y at $\alpha = -27^\circ$).

Table 2 – Model partitioning with the full store model as base model used to generate sub-models 2 and 3.

X Designation	Sub-Model Designation	Model/Sub-Model	X termination [m]
Full Store LNOSE +LCENTRE+LAFT	1	•	3.239
LNOSE+LCENTR	2	•	2.631
LNOSE	3	•	0.762

Table 3 – Missile DATCOM aerodynamic model segment definition for the large finned store.

Segment Designation Name	Segment Designation	Model Segment	X reference [m]
Aft Body	C = 1 - 2	·	2.934
Centre Body	B = 2 - 3	•	1.696
Nose Cone	A = 3	•	0.254

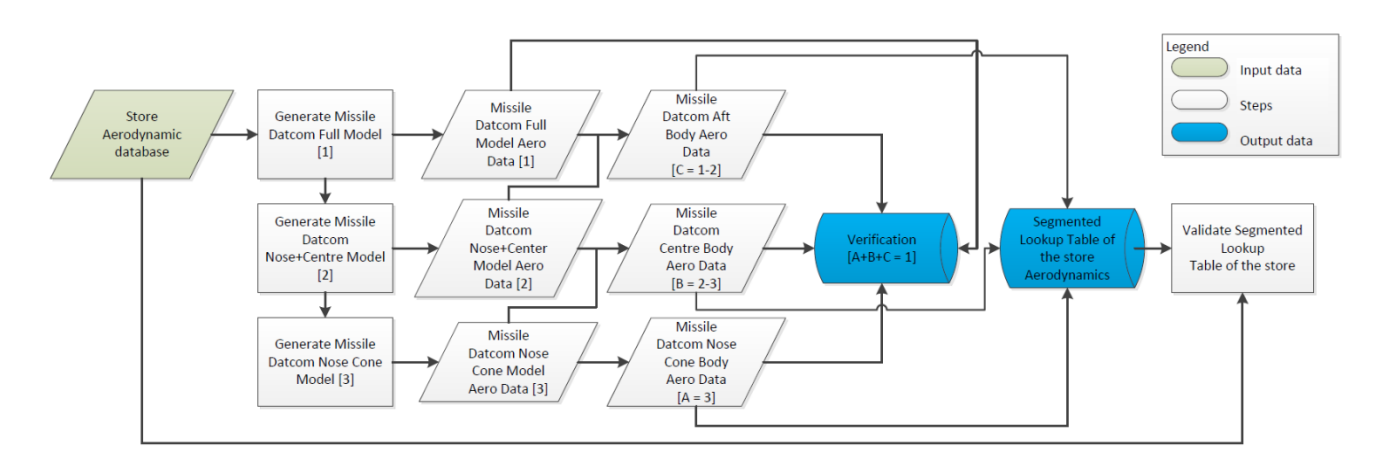
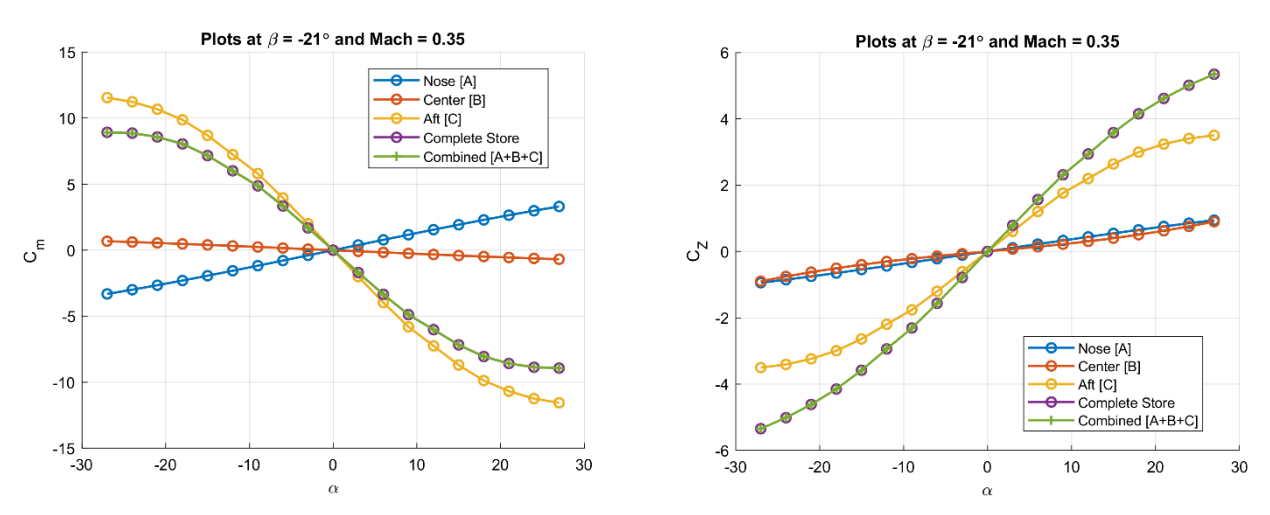
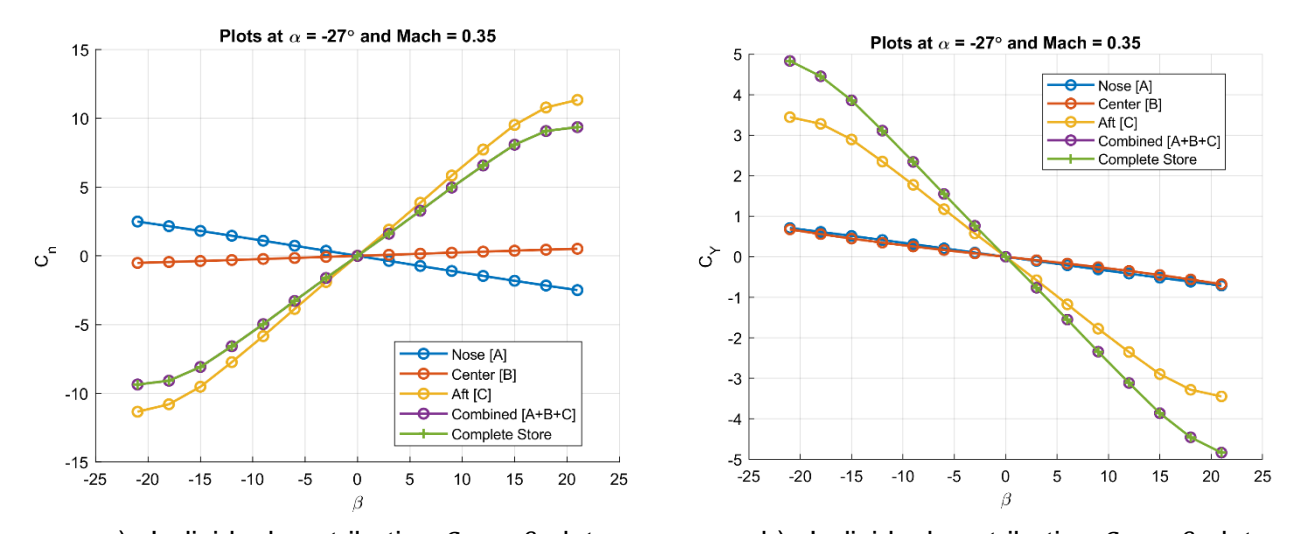


Figure 5 – Look-up table generation using MATLAB script flowchart.



a) Individual contribution C_m vs α plots b) Individual contribution C_Z vs α plots Figure 6 – Typical build-up of store components, C_m vs α and C_Z vs α for $\beta = -21^\circ$.



a) Individual contribution C_n vs β plots b) Individual contribution C_Y vs β plots Figure 7 – Typical build-up of store components, C_n vs β and C_Y vs β for $\alpha = -27^\circ$.

2.2.2 CFD Modelling

The aircraft velocity flow field was calculated using Star-CCM+ (Version 2210, Build 17.06.007), a commercial CFD solver. The solver was run on a Dell Precision 7770 workstation with a 12th generation Intel Core $^{\text{TM}}$ i7-12850HX processor and 132 Gb of RAM. This section contains a description of the domain that was used, the mesh, and finally the solver.

Geometry

A schematic and dimensions of the parent aircraft from which a three-dimensional model was created are shown in Figure 3. As a solution of the flow field around the aircraft was sought, the volume of air bounding the aircraft was modelled as a rectangular prism with length, width, and breadth equal to sixty times the length, width, and breadth of a similar rectangular prism bounding the parent aircraft as partially illustrated in Figure 8. The nose of the parent aircraft was set to nine times the length of the aircraft from the inlet boundary.

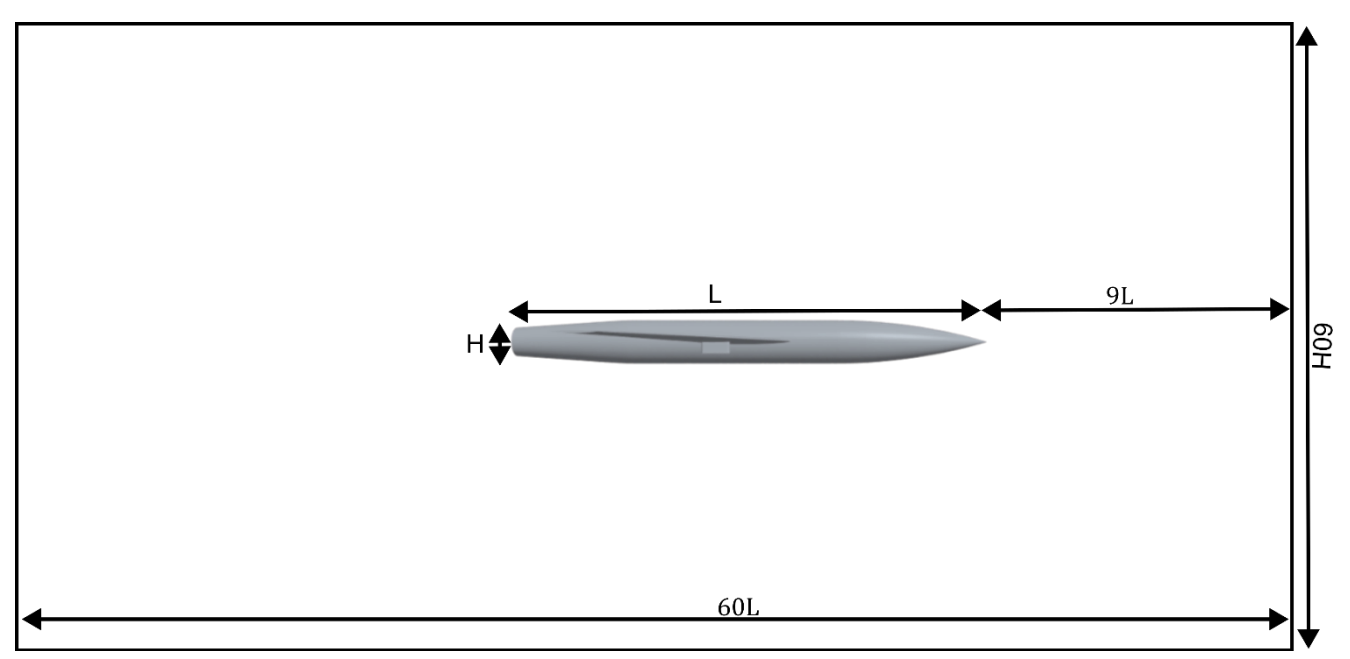


Figure 8 – Domain extent that was used to calculate the velocity flow field around the parent aircraft with L = 18.51 m and H = 1.69 m as shown in Figure 3. The width was 60 times the wingspan of the aircraft (720 m).

With the domain established, a polyhedral mesh was created based on a reference length of L. The minimum and maximum cell sizes on the surface were set at 0.08 % and 0.5 %, respectively. The

growth rate between the smallest and largest cell was 1.1. A layer of ten prism cells was placed near the wall boundaries to resolve boundary layers. Prandtl's flat plate theory was used to estimate the total thickness of the boundary layer and hence prism layers. The thickness of the first layer was also calculated with the requirement that the Y+ value should be equal to one [22]. The cell size of the outer boundary of the domain was fixed at 30 % of the reference length. Finally, the volume was filled with polyhedral cells growing from the surface to the outer boundary at a volume growth rate of 1.05 and the wake behind the aircraft for up-to three times the reference length was refined to 0.5 % of the reference length. The errors due to this discretisation were assessed using Roache's method [23] and the results presented below. A view of a typical mesh is shown in Figure 9.

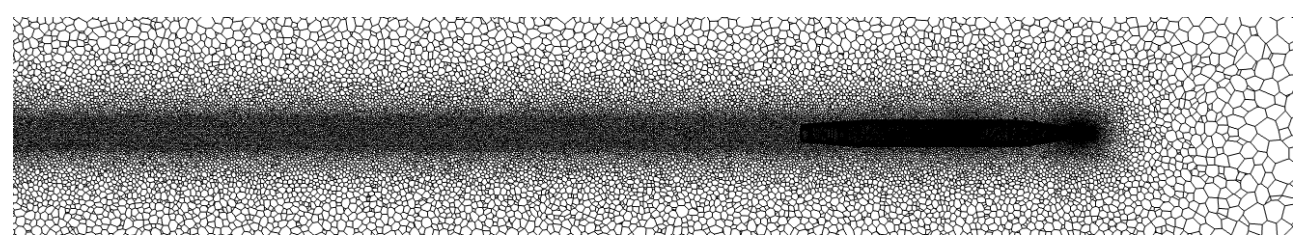


Figure 9 – A view of the base mesh that was used to calculate the velocity flow field.

Physics and Solver Setup

Star-CCM+ uses the finite volume formulation to calculate numerical solutions of the Reynolds averaged Navier-Stokes (RANS) equations shown in Equations 1 to 3. In Equations 1 to 3, ρ , σ , E, f_b , q, and S_E represent fluid density, velocity flow field, the stress tensor, energy, body forces, heat flux, and energy sources per unit volume. However, the latter three terms were not modelled as they are not relevant to the current work.

$$\frac{\partial \rho}{\partial t} + \nabla \cdot \rho = 0 \tag{1}$$

$$\frac{\partial \rho}{\partial t} + \nabla \cdot \rho = 0 \tag{1}$$

$$\frac{\partial (\rho v)}{\partial t} + \nabla \cdot (\rho v v) = \nabla \cdot \sigma + f_b \tag{2}$$

$$\frac{\partial(\rho E)}{\partial t} + \nabla \cdot (\rho E v) = f_b \cdot v + \nabla \cdot (v \cdot \sigma) - \nabla \cdot q + S_E$$
(3)

For closure the fluid was assumed to be air and modelled as an ideal gas with viscosity following Sutherland's law. Turbulence was modelled using the SST k-ω model, a modification of the standard k-ω model which corrects for the sensitivity of the inlet conditions on turbulent kinetic energy (k) and specific dissipative rate (ω) [21]. However, as shown by the grid convergence study below and a comparison of inviscid and viscous results in the discussion of subsection 4.1, it is sufficient to use an inviscid model to estimate the flow field.

The coupled flow solver in Star-CCM+ was then used to calculate the numerical solution of the conservation Equations 1-3 above, assuming a steady state exists. The second order upwind scheme was used to calculate convective fluxes. Flow conditions in Roberts and Myers [18] were used to set the freestream boundary to Mach 0.4 at an altitude of 5000 ft assuming the international standard atmosphere (ISA) model [24]. The Courant (CFL) number was set to vary linearly from 0.1 to 30 over the first 500 iterations. A small CFL number helps maintain solver stability when transients dominate the flow field while a larger CFL number later ensures faster convergence. The solver was considered converged when the monitored quantity (drag) approached an asymptote with normalised variations of at-most 0.01 over 100 iterations.

Table 4 – Coordinates of the points that form the sampling grid illustrated in Figure 1.

X (m)	0	0.508	1.016	1.524	2.032	2.540	3.048	3.556	4.064	4.572
<i>Y</i> (m)	-1.016	-0.750	-0.508	-0.254	-0.075	0.075	0.254	0.508	0.750	1.016
Z (m)	-4.115	-3.454	-2.445	-1.778	-1.422	-0.965	-0.66	-0.356	-0.152	0

When the solver converged, the velocity flow field below the parent aircraft was resampled. The sampling grid was composed of 1000 points spread uniformly in the x and y-directions. Figure 1

shows x, y, and z positions with the origin at (8.128, 2.032, -0.229) m relative to the nose of the parent aircraft. The grid was formed from a permutation of these positions. In the z-direction, the point density decreased monotonically with increasing distance from the parent aircraft.

Grid Convergence Study

A grid convergence study was conducted to assess the influence of discretisation as described by Roache [23]. The output from this study was a grid convergence index (GCI) representing the error due to the grid. The GCI is calculated according to Equation 4 where ϵ is the absolute difference between the measured quantity calculated using two different grids of varying coarseness; r is the refinement factor; and p is the order of the CFD algorithm. In this instance, a second order algorithm was used.

$$GCI = \frac{\epsilon}{1 - r^p} \tag{4}$$

Table 5 – Grid convergence indices for five refinement levels calculated using drag compared to flow speed at three sampling points: $P_1(0, -1.016, -6.401)$ m, $P_2(4.572, -0.75, -4.115)$ m, and $P_3(4.572, -6.401)$ m, $P_3(4.572, -6.401)$ m, $P_3(4.572, -6.401)$ m, $P_3(4.572, -6.401)$ m, $P_3(4.572, -6.401)$ m, and $P_3(4.572, -6.401)$ m, $P_3(4.572, -6.401)$ m, P0.75. -0.965) m. Δx is the smallest represents the smallest cell in the domain.

	6.76, 6.666) III. Dx is the sindhest represente the sindhest centri the demain.										
Case	#Cells	Δx (m)	Drag (N)	ΔDrag	GCI	<i>V_{P1}</i> (m/s)	V _{P2} (m/s)	<i>V_{P3}</i> (m/s)	Wall Time (s)		
0	5162408	4.00e-3	12335.4	1	-	132.95	132.73	132.45	1861		
1	5769406	3.50e-3	11983.1	2.86%	12.18%	133.00	132.70	132.46	2000		
2	6614486	3.00e-3	11719.8	2.20%	8.28%	133.00	132.72	132.36	2300		
3	8607569	2.25e-3	11269.3	0.33%	8.79%	133.02	132.74	132.50	2918		
4	9648364	2.00e-3	11253.0	0.14%	0.49%	132.94	132.67	132.36	3065		

The results of the grid convergence study are shown in Table 5 where the velocity at the sampling points does not vary significantly. This is because the sampling points are distributed away from the influence of the parent aircraft and are therefore closer to the free stream. Drag, on the other hand, can be seen to approach an asymptote as the grid is refined. Based on Table 5, it is plausible to use the coarse mesh (such as Case 0) to estimate the velocity field at the sampling points. This, because grid refinement does not seem to influence velocity flowfield in the region of interest while increasing the computation time involved.

2.2.3 Trajectory Calculation

A 6-DOF rigid body model (Equations 5 and 6) in the ARUV code was used to calculate the store trajectory. ARUV is a low-order panel code with a fixed wake and an extensive array of features supporting store separation analyses. It is a further development of the USTORE code [11] developed by the CSIR and which is described in detail in [8]. Equation 5 where m, t, and v represent store mass, time, and store velocity describes how the store translates. Similarly, Equation 6 represents the store's rotation about the store's body reference frame with the origin at the store's centre of mass. M, ω , and n represent the store's moments of inertia tensor; angular velocity vector; and resultant store moments.

$$m\frac{d\mathbf{v}}{dt} = \mathbf{f}_{\mathbf{b}} \tag{5}$$

$$m\frac{d\mathbf{v}}{dt} = \mathbf{f}_{b}$$

$$M\frac{d\boldsymbol{\omega}}{dt} + \boldsymbol{\omega} \times M\boldsymbol{\omega} = \mathbf{n}$$
(6)

Mass and moments of inertia of the store are shown in Table 6. The off-diagonal components of the inertia tensor were all zero. Table 6 also shows the initial velocity and attitude of the store. The resultant body forces and moments were calculated using the sampled flow field, the store aerodynamic properties from Missile Datcom and the local motion of the reference point of each store segment, resulting in a closed set of Equations 5 and 6. The equations were numerically integrated using the Kutta-Merson method to calculate the store's trajectory and attitudes. The results are compared to Roberts and Myers [18] wind tunnel results in Section 3 below.

Note that using the local motion at each store segment's reference point to adjust the local flow condition allows the approximation of the store's plunging and angular aerodynamic damping properties to be approximated in the trajectory dynamics, something that is not possible in non-segmented store models.

2.3 Methodology verification test case

2.3.1 Test Case Description

Table 6 lists the four AEDC-TR-73-87 wind tunnel trajectory test cases that were identified as suitable candidates to validate the proposed methodology by comparison with the FastTraj simulation result. Tests were conducted at $M_{\infty} = 0.4$ and Re = 3.6 million per foot, and aircraft angles of attack of 0° and 6°. The full-scale store has a mass of 56.66 kg and 226.64 kg and the center of mass is located at the store mid-body. The store has a 45-degree roll orientation at the pylon position (0, 0, 45) and ejection velocities of 3.048 m/s (0, 0, -3.048) relative to the aircraft axes. The store translation and orientation data were compared for a wing-mounted store release.

Table 6 – AEDC-TR-73-87 wind tunnel trajectory test cases for comparison with FastTraj [18].

	Aircraft flight condition					Store mass properties			
Test Configuration	H [ft]	<i>M</i> ∞ [-]	ψ_{ac} [deg]	$lpha_{ac}$ [deg]	ϕ_{ac} [deg]	m [kg]	I_{XX} [kg.m 2]	$I_{\gamma\gamma}$ [kg.m²]	I_{ZZ} [kg.m 2]
T-400	5000	0.4	0	0	0	56.66	2.7120	27.117	27.117
T-401	5000	0.4	0	6	0	56.67	2.7130	27.117	27.117
T-403	5000	0.4	0	0	0	226.65	10.848	108.466	108.467
T-405	5000	0.4	0	6	0	226.67	10.850	108.466	108.467

The tests were conducted in the closed loop, continuous flow, variable-density, Aerodynamic Wind Tunnel (4T) at the Arnold Engineering Development Centre (AEDC) in Tennessee, USA, in 1974. The aircraft-store was a 5% scaled wind tunnel model. The store model was a Stable Store, referred to as Large Force Finned (LFF), with rectangular planform fins and is mounted on the wing station. The aircraft model has 45° wing sweep at the quarter-chord line, an aspect ratio of 4, a taper ratio of 0.3 and 6 % thick symmetric aerofoil sections. Sketches of the full-scale wing-fuselage model and store are shown in Figure 3. Two separate and independent model support systems were used during the test. The parent model was inverted in the test section and supported by an offset sting attached to the main pitch sector that allows for pitch control. The store model was supported by the Captive Trajectory Support (CTS) system. The CTS system provides store movement with 6-DOF, independent of the parent aircraft model. A digital computer is programmed to solve the 6-DOF equations to calculate the angular and linear displacements of the store relative to the aircraft pylon. This calculation involves using the measured static aerodynamic coefficient values to calculate the new position and attitude of the store. The CTS is then commanded to move the store model to this new position and the aerodynamic loads are measured again for the next 6-DOF calculation. This process is repeated until a full trajectory has been acquired.

2.3.2 Test case data precision

Table 7 lists the estimated uncertainties in model and probe positioning. According to Roberts and Myres [18] these uncertainties are the consequence of the CTS and main pitch sector's ability to accurately set a specified parameter.

Table 8 lists the estimated uncertainties in the force model data which considers the probable inaccuracies in the balance measurements and tunnel conditions.

Table 9 lists the estimated uncertainties in store translational and angular displacements. According to Roberts and Myers [18], these are the maximum estimated uncertainties that result from errors in

translational and angular placements, extrapolation tolerances, and balance accuracy. The light store linear and angular displacement errors are substantially more compared to those of the heavy store. Due to its smaller mass and inertial properties, it is more aerodynamically sensitive and has less damping characteristics.

Table 7 – Estimated uncertainties in model and probe positioning.

$\Delta X[m]$	$\Delta Y[m]$	$\Delta Z[m]$	$\Delta \alpha_{store} [deg]$	$\Delta \alpha_{aircraft} [deg]$
±0.00152	±0.00152	±0.00152	±0.15	±0.10

Table 8 – Estimated uncertainties in the force model data.

M_{∞}	ΔM_{∞}	$\Delta q_{\infty} [Pa]$	ΔC_N	ΔC_Y	ΔC_m	ΔC_n	ΔC_A
0.4	±0.005	±2.2	±0.02	±0.02	±0.03	±0.03	±0.05

Table 9 – Estimated uncertainties in store translational and angular displacements.

M_{∞}	$m_{store}[kg]$	t [s]	$\Delta X [m]$	$\Delta Y[m]$	$\Delta Z[m]$	$\Delta \theta_{store} [deg]$	$\Delta\psi_{store}$ [deg]
0.4	56.66	0.5	±0.081	±0.054	±0.024	±1.9	±4
0.4	226.64	0.5	±0.021	±0.012	±0.006	±0.5	±1

3. Results

3.1 6-DOF model Co-ordinate System

The 6-DOF aircraft-store model reference coordinate system is a right-handed co-ordinate system. The $0_{x,body}$ axis is positive rearwards, the $0_{y,body}$ axis points to starboard, and the $0_{z,body}$ axis is directed upwards as shown in Figure 10 below. The aircraft-store linear translations are positive when their direction of action is the same as the direction of the axis to which they relate. Positive roll is left wing down or roll to the left. Positive pitch is nose up. Positive yaw is nose to the left.

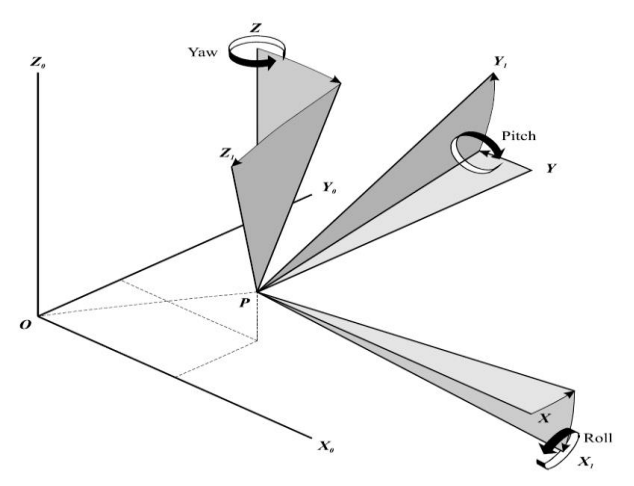


Figure 10 – 6-DOF Aircraft-store model reference coordinate system

3.2 Verification cases

The FastTraj method is verified by comparing the calculated trajectory against the Roberts and Myers [18] wind tunnel data. The store translations and orientations were compared for a wing-mounted store release. Figure 11 through Figure 14 below compare the store trajectory calculated with the FastTraj methodology and digitised trajectory data by Roberts and Myers [18]. The store translational and angular displacement uncertainties in the AEDC wind tunnel data listed in

Table 9 have been plotted. Figure 11 and Figure 12 show that the angular displacements are within the experimental data error band for the light store and correlate well with the trends and magnitude of the trajectory. However, there are notable deviations seen in the initial part of the trajectory up to a maximum of 12.5% and 10%, respectively, for the pitch and yaw orientation between 0.1-0.3 s for the

T-400 test case and a maximum deviation of 9.2% and 7.6% for the pitch and yaw angular displacements, respectively, between 0.1-0.3 s for the T-401 test case.

Figure 11 and Figure 12 show that the calculated linear translations are largely within the experimental data error band and correlate well with the expected trajectory trends and magnitudes except for the axial and vertical translation in case T-400 and vertical translation in case T-401 which show a maximum deviation of 10%, 3% and 13%, respectively between 0.5-0.6s. The results for cases T-400 and T-401 demonstrate that FastTraj can accurately predict store trajectories for release configurations where the light store dynamics are dominated by aerodynamic forces. As seen in Figure 11 and Figure 12, the angular displacements show that the store is more aerodynamically sensitive compared to the heavy store as shown in Figure 13 and Figure 14.

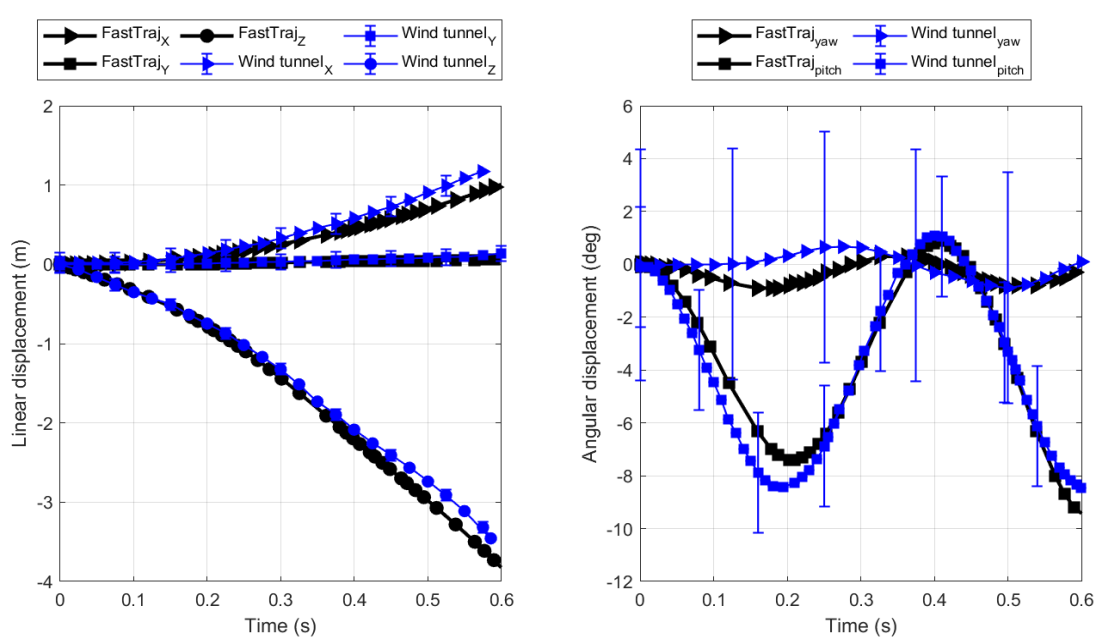


Figure 11 – Store translation and orientation relative to the store origin at the wing pylon station for the T-400 test case.

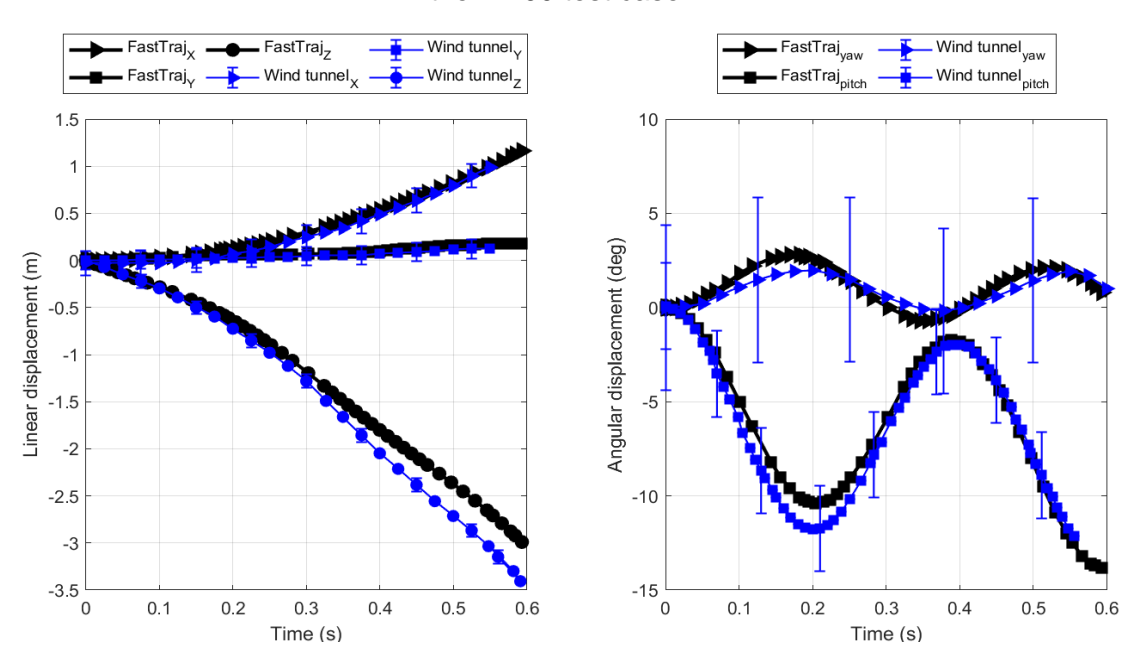


Figure 12 – Store translation and orientation relative to the store origin at the wing pylon station for the T-401 test case.

Figure 13 and Figure 14 show that the calculated linear translations for the heavy store are largely within the experimental data error band and correlate well with the expected trajectory trends and magnitudes from the reference data except for the axial translation in case T-405 which shows a

significant deviation compared to wind-tunnel data. The cause of this deviation is unknown and requires further investigation, however, it is inconsistent with the other case studies (T-400, T-401 and T-403) which show a maximum deviation of 10 % for the store axial translation.

Figure 13 and Figure 14 also show that the angular displacements are within the experimental data error band and correlate well with the observed trends and magnitude of the trajectory in the reference data. Compared to experimental result, the respective pitch and yaw orientations show a maximum deviation of 3.2% and 4.0%, for case T-403 and 4.0% and 9.2%, for case T-405. The results for cases T-403 and T-406 exhibit that FastTraj can be used to predict store trajectories for release configurations where the store inertial properties dominate its aerodynamics. As seen in Figure 13 and Figure 14, the angular displacements show that the store is less aerodynamically sensitive compared to the light store as shown in Figure 11 and Figure 12.

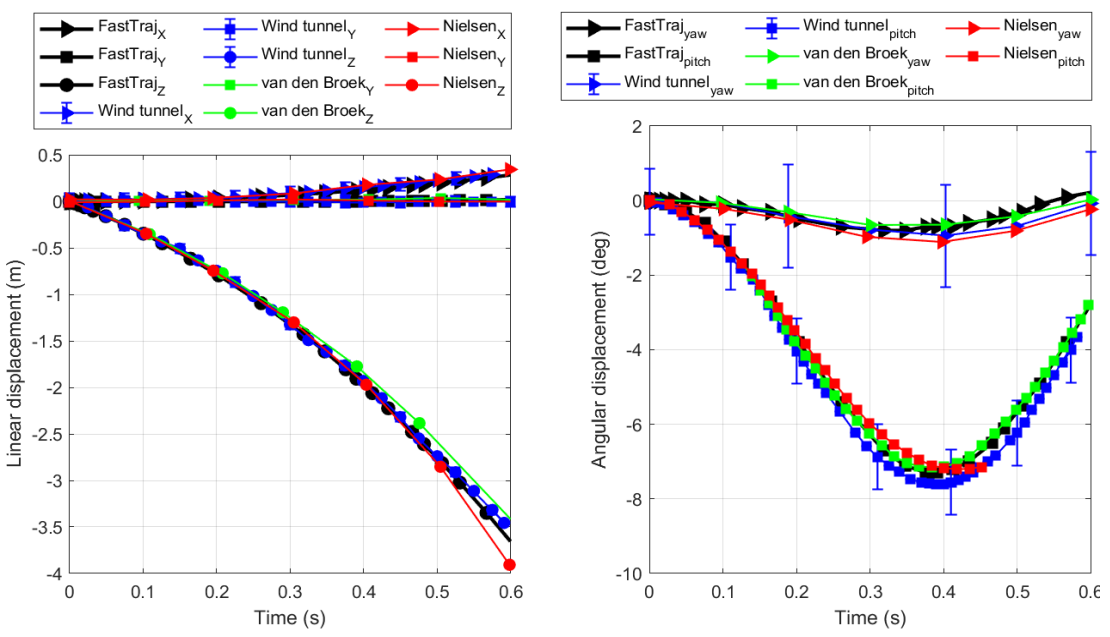


Figure 13 – Store translation and orientation relative to the store origin at the wing pylon station for the T-403 test case.

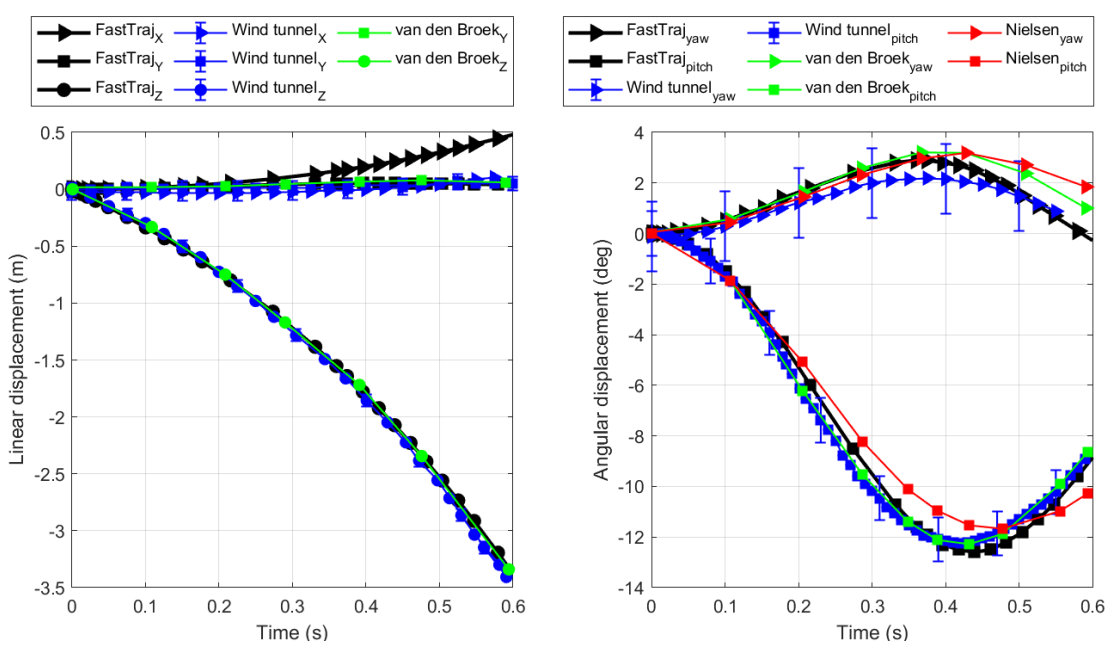


Figure 14 – Store translation and orientation relative to the store origin at the wing pylon station for the T-405 test case.

4. Discussion

This section highlights the unique characteristics of the FastTraj methodology that allow for rapid and accurate estimation of store linear and angular displacements in the low subsonic flight regime. It has been mentioned in subsection 1.2, that for the low subsonic flight regime, the mutual influence that the aircraft and store exert on each other is small enough that the store release modelling can reasonably assume that their aerodynamics are decoupled. This allows for independent modelling of the aircraft and the store aerodynamics.

4.1 Inviscid modelling of aircraft aerodynamics

The assumption of inviscid compressible flow was made to speed-up the computation of the aircraft flow field. Compared to the transonic flow regime, the influence of the aircraft's viscous boundary layer aerodynamics is limited to a narrow region on the aircraft in the low subsonic flow regime, and thus has a small effect on the store separation aerodynamics. Furthermore, the release position of the store is usually on a pylon outside of the aircraft viscous boundary layer, where the flow can be considered inviscid. Stores are normally released when the parent aircraft is not stalled, with attached airflow prevailing.

A comparison of the flow field based on both viscous and inviscid models in Figure 15 and Figure 16 shows their absolute difference in flow field speed. As expected, the largest difference, albeit negligible, occurs near the aircraft and close to the pylon (located between 9 and 10 m from the nose). It is based on this observation that it was considered plausible to use inviscid flow fields.

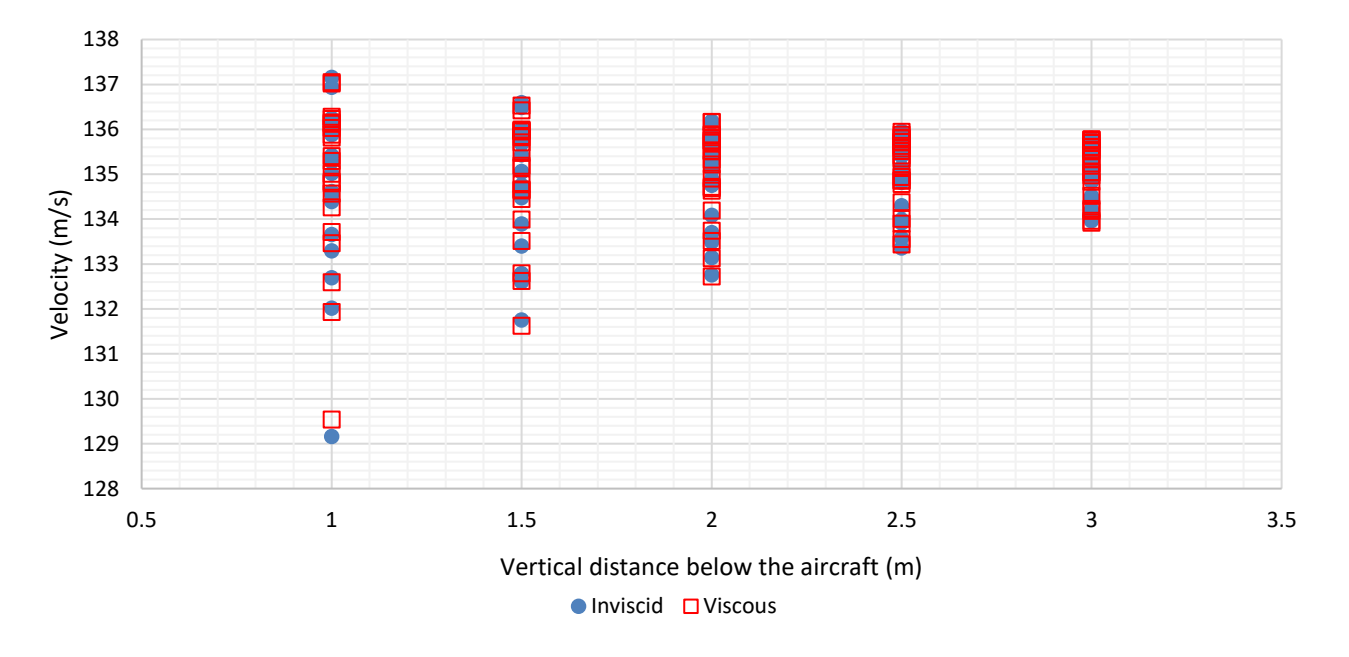


Figure 15 – A comparison of the velocity components calculated using inviscid and viscous models.

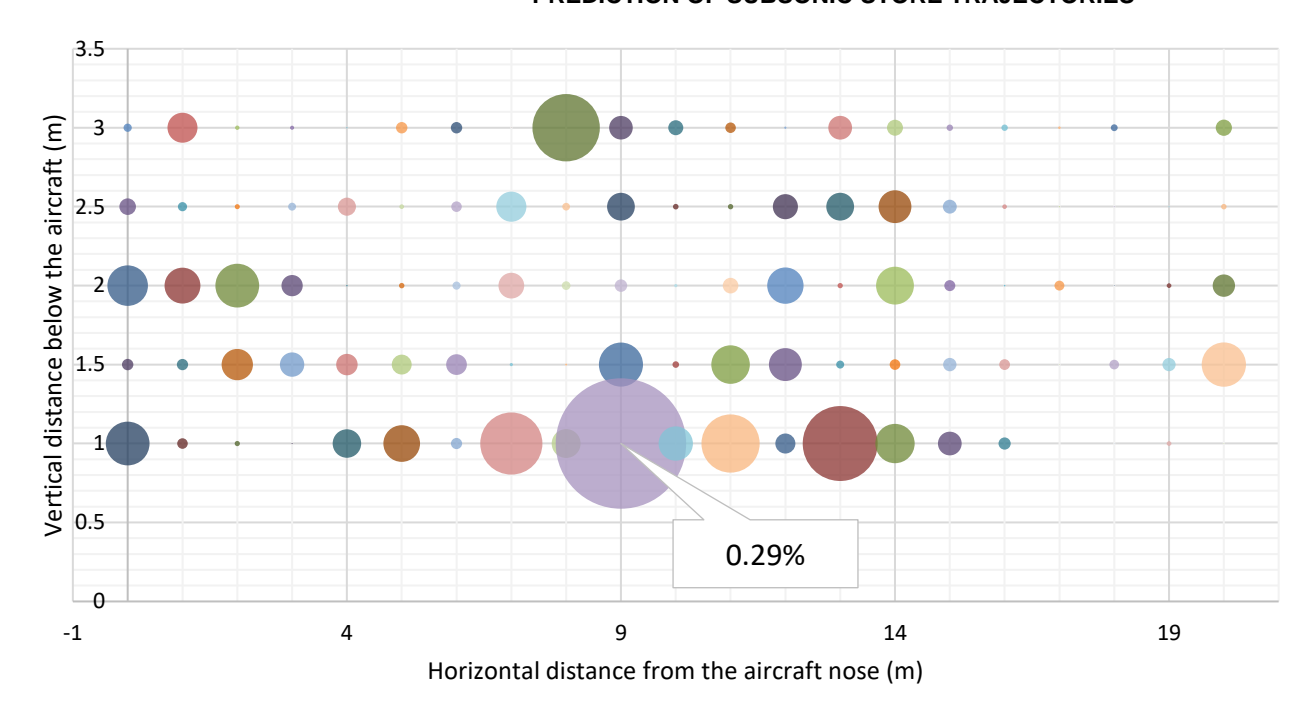


Figure 16– Percentage difference between viscous and inviscid models of sampled flow field speed below the parent aircraft. Bubble diameter is proportional to the percent difference.

4.2 Aerodynamics loads look-up table correction

The 6-DOF model requires a store aerodynamics loads database as input to the store release calculation. This aerodynamic database can be obtained from any source, experimental or computational. In this case, Missile Datcom was used, however, a correction was required to match its data with a prediction by a high-fidelity CFD model. Missile Datcom software is capable of approximately calculating the aerodynamic trends of a store in isolation, however, it tends to overpredict and, in some instances, underpredict the magnitudes, affecting the slope of the aerodynamic curves. This leads to inaccurate predictions of the released store trajectory. This source of inaccuracy is overcome by an application of a linear correction factor to adjust the slopes to match high-fidelity CFD results. The correction effort only required a few flight maneuver points to be modeled in CFD as follows:

- 1. $0 \deg < \alpha < 24 \deg$ at 6 deg increments for an $\beta = 0$.
- 2. $0 \deg < \beta < 24 \deg$ at 6 deg increments for an $\alpha = 0$.

Figure 17 and Figure 18 show the outcome of the correction process and Table 10 list the correction factors that were applied for the various aerodynamic coefficients.

Table 10 – Store aerodynamic coefficient correction factor.

Store aerodynamic coefficient	C_A	C_Y	C_N	C_l	C_m	C_n
Correction factor	1.1	0.85	0.85	1.0	0.85	0.85

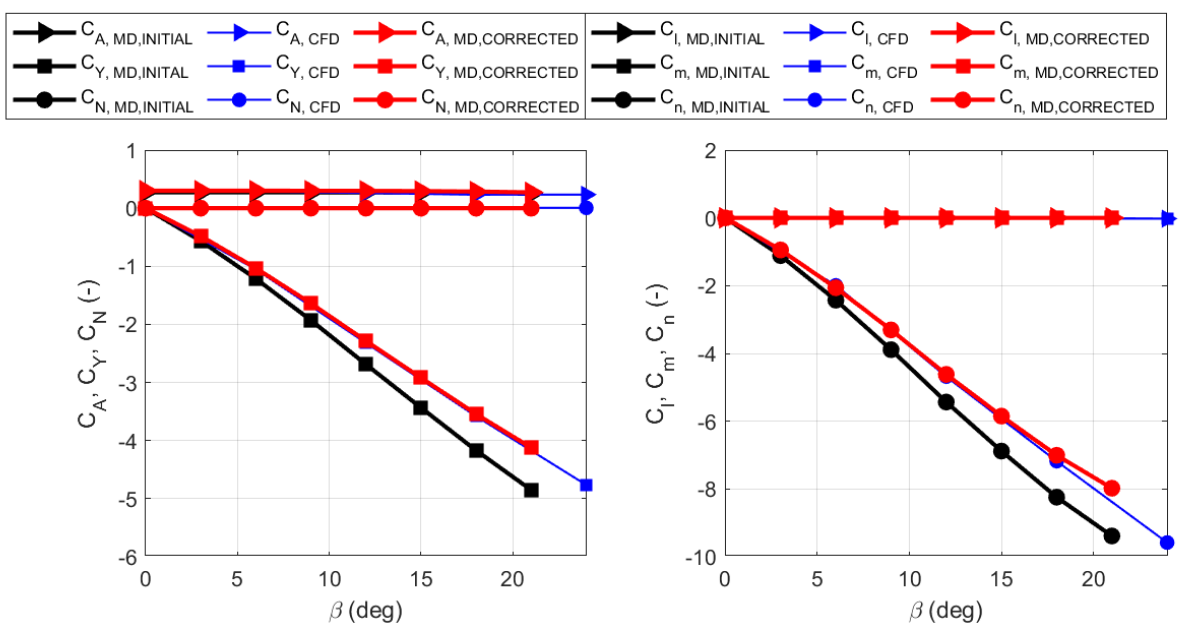


Figure 17 – Missile Datcom store aerodynamic coefficient correction to match high-fidelity CFD model result for an Angle of Attack sweep and zero Angle of Sideslip.

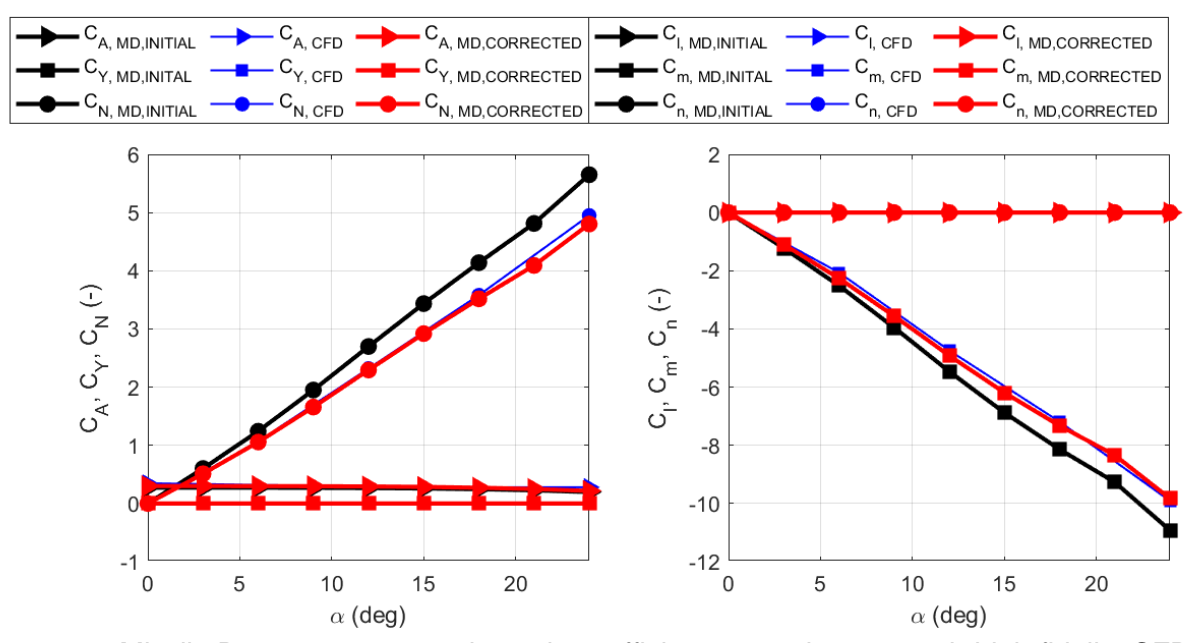


Figure 18 – Missile Datcom store aerodynamic coefficient correction to match high-fidelity CFD model result for an Angle of Sideslip sweep and zero Angle of Attack.

Segmenting the aerodynamics look-up table is necessary as discussed in subsection 4.3. This process is performed using Missile Datcom, making this software an integral part of the FastTraj methodology. In general, any verified store aerodynamic model can be segmented with useful accuracy by making use of Missile Datcom.

4.3 Segmented aerodynamics loads look-up table

To capture the flow field influence on the store along its longitudinal axis, the store aerodynamics look-up table is segmented into three segments, viz., nose, mid and tail body, as discussed in subsection 2.2.1. This allows for an accurate representation of the store's aerodynamic damping characteristics by the aerodynamics model; and Figure 19 and Figure 20 Figure 19 illustrates the effect of this modeling approach for the light and heavy store. The store linear displacements are comparable to the reference data and the FastTraj result based on the segmented aerodynamics

look-up table shown in Figure 11 and Figure 13Figure 13. However, Figure 19 and Figure 20 Figure 19andFigure 20 also show that the store pitch angular displacement deviates significantly from the reference data and the FastTraj result based segmented aerodynamics look-up table. The yaw orientation result indicates different lateral characteristics for the T-400 test case, however, it is only marginally affected for the T-403 test case. The differences between the trajectories of the segmented and non-segmented models show the importance of the method's ability to capture the changes in the aircraft flow field along the length of the store. This result emphasises the need to segment the aerodynamics look-up table to better capture the store's angular dynamics as the effect of the flow field variations along the length of the store are significant.

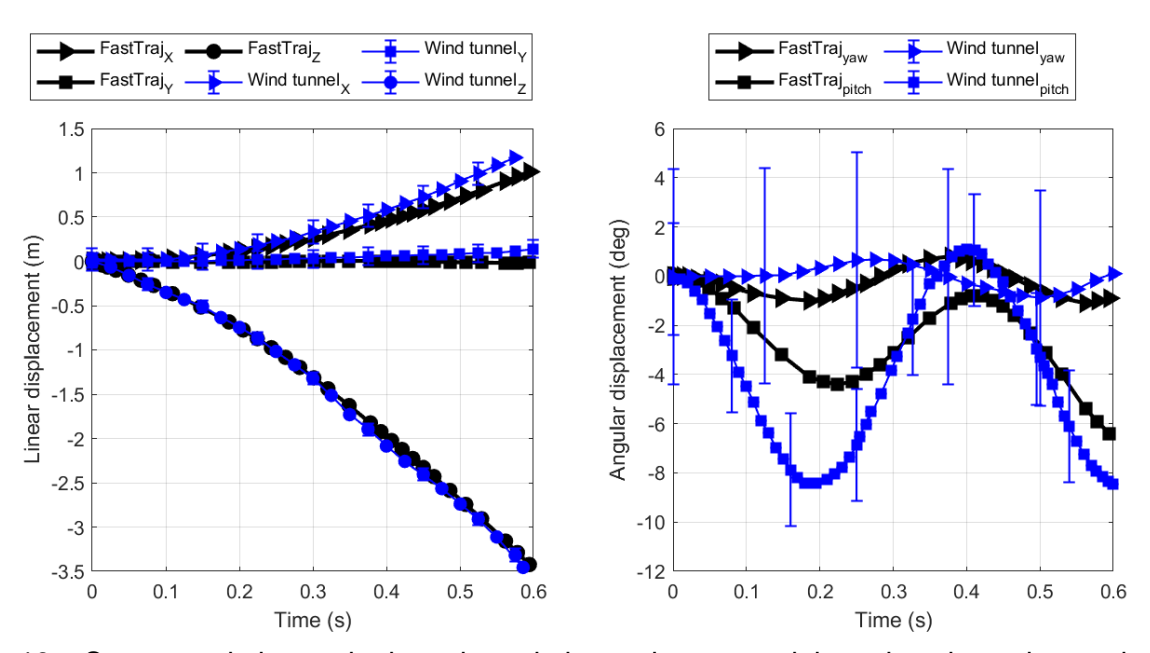


Figure 19 – Store translation and orientation relative to the store origin at the wing pylon station for the T-400 test case based on the non-segmented aerodynamic look-up table.

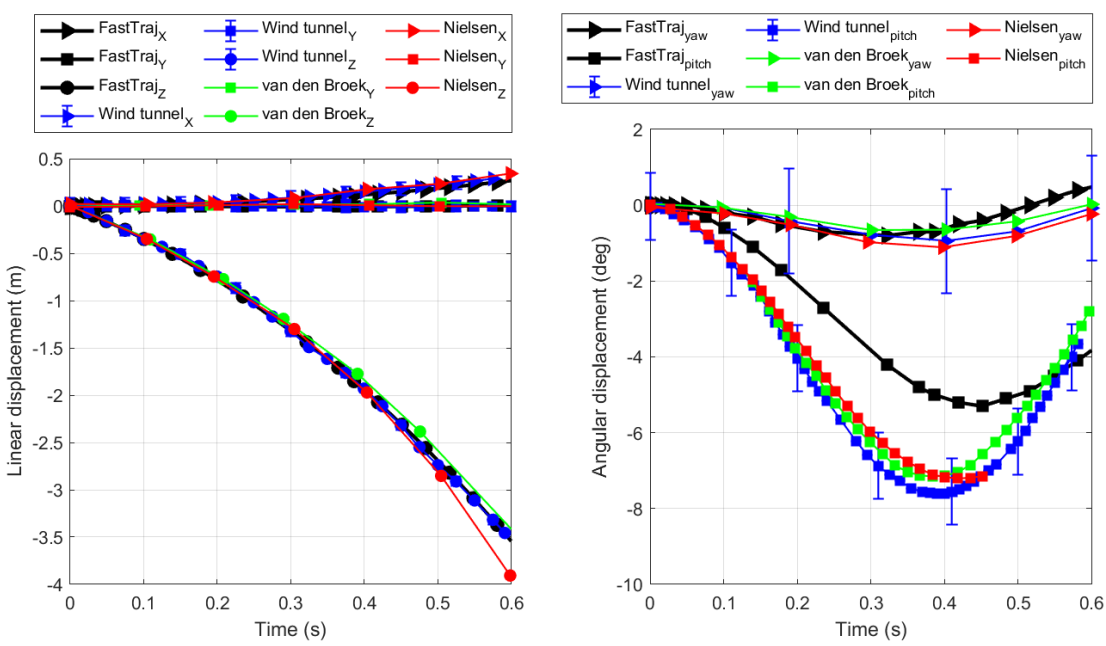


Figure 20 – Store translation and orientation relative to the store origin at the wing pylon station for the T-403 test case based on the non-segmented aerodynamic look-up table.

5. Conclusions

The FastTraj subsonic store separation analysis method was described and demonstrated using a wind-tunnel test case. This method aims to maximise store separation analysis productivity while still producing accurate trajectories. Modern CFD models are quicker to set up from CAD models than legacy panel codes like ARUV. Using inviscid CFD in a decoupled manner is shown to produce good results proving that in many cases the computational expense of time accurate RANS analyses is not justified for subsonic store separation analyses. Inviscid CFD requires a smaller and simpler mesh and is significantly quicker to solve, enabling more separation scenarios to be studied. It was demonstrated that it is necessary for the store model to at least be segmented to capture flow field perturbations along the length of the store. The wind-tunnel test case did not include store aerodynamic damping effects and it is recommended that the use of segmented store models to capture aerodynamic damping effects in separation trajectories be investigated using suitable experimental data.

6. Contact Author Email Address

Mailto: nmthembu1@csir.co.za.

7. Author Responsibilities

Kevin Jamison conceived the method and the study. The work was then split equally among the rest of the authors. The results were discussed by all authors. Hlamulo Ndlovu developed the MATLAB script that was used with Missile Datcom to generate the aerodynamic properties of the segmented store; Bright Ndebele completed the CFD study that generated the flow field around the parent model; Ndumiso Mthembu performed the 6-DOF trajectory calculations; and Lindokuhle Zwane completed the literature survey.

8. Copyright Statement

The authors confirm that they, and/or their company or organization, hold copyright on all the original material included in this paper. The authors also confirm that they have obtained permission, from the copyright holder of any third-party material included in this paper, to publish it as part of their paper. The authors confirm that they give permission or have obtained permission from the copyright holder of this paper, for the publication and distribution of this paper as part of the ICAS proceedings or as individual off-prints from the proceedings.

References

- [1] North Atlantic Treaty Organization. Aerodynamics of Store Integration and Separation. *AGARD-CP-570*, Advisory Group for Aerospace Research and Development (AGARD), *76th Fluid Dynamics Panel Symposium*, Ankara, Turkey, 1996.
- [2] Cenko A. Store separation lessons learned during the last 30 years. 27th International Congress of the Aeronautical Sciences, Nice, France, 2010.
- [3] North Atlantic Treaty Organization. Aircraft/stores compatibility, integration and separation testing. *STO-AG-300-V29*, Science and Technology Organization (STO), 2014.
- [4] Schindel L.H. Store separation. *AGARD-AG-202*, Advisory Group for Aerospace Research and Development (AGARD), North Atlantic Treaty Organization, 1975.
- [5] Department of Defense. Aircraft/stores compatibility: systems engineering data requirements and test procedures. MIL-HDBK-1763, USA, 1998.
- [6] Department of Defense. Guide to aircraft/stores compatibility. MIL-HDBK-244A, USA, 1990.
- [7] Jamison K, Rossouw P and Miles E. Quantitative grading of store separation trajectories. *AIAC-2017-153*, *9th Ankara International Aerospace Conference*, METU, Ankara, Turkey, 2017.
- [8] Jamison K. Grid-mode transonic store separation analyses using modern design of experiments. 31st Congress of the International Council of the Aeronautical Sciences, Belo Horizonte, Brazil, 2018.
- [9] Panagiotopoulos E.E and Kyparissis S.D. CFD transonic store separation trajectory predictions with comparison to wind tunnel investigations. *International Journal of Engineering (IJE)*, Vol. 3, Issue 6, pp 538-553, 2010.
- [10]Synder D.O, Koutsavdis E.K and Anttonen J.S.R. Transonic store separation using unstructured CFD with dynamic meshing. *AIAA* 2003-3919, 33rd AIAA Fluid Dynamics Conference and Exhibit, Orlando,

Florida, 2003.

- [11]van den Broek G.J. The Use of a Panel Method in the Prediction of External Store Separation. *Journal of Aircraft*, Vol. 21, No. 5, pp 309-315, 1984.
- [12]Peters M, Wissink A and Ekaterinaris J. Machine learning-based surrogate modeling approaches for fixed-wing store separation. *Aerospace Science and Technology*, 2023
- [13] Davids S and Cenko A. Grid based approach to store separation. *AIAA 2001-2418. 19th AIAA Applied Aerodynamics Conference*, 2001.
- [14]Demir G and Alemdaroğlu N. CFD based solutions of release of a transonic generic store. *AIAC-2019-1094, 10th Ankara International Aerospace Conference, METU, Ankara, Turkey, 2019.*
- [15] Cenko A, Meyer R and Tessitore F. Further development of the influence function method for store aerodynamic analysis, *Journal of Aircraft*, Vol. 23, No. 8, pp 656-661, 1986.
- [16] Morgret C, Smith M and Moore D. The FLIP 4 store-separation trajectory simulation code. *AIAA 2009-100, 47th AIAA Aerospace Sciences Meeting including The New Horizons Forum and Aerospace Exposition*, Orlando, Florida, 2009.
- [17] Sickles W.L. CFD in support of wind tunnel testing for aircraft/weapons integration. *HPCMP Users Group Conference*, Williamsburg, Virginia, United States of America, 2004.
- [18]Roberts R. H. and Myers J. R. Flow-field characteristics and aerodynamic loads on external stores near the fuselage and wing-pylon positions of a swept-wing/fuselage model at Mach numbers of 0.4 and 0.7 Phase V, Arnold Engineering Development Center, USAF, AEDC-TR-73-87, 1974.
- [19]Siemens Digital Industries Software, "Simcenter STAR-CCM+ documentation," 2022.
- [20]Blake W.B. Missile DATCOM: User's Manual—1997 Fortran 90 Revision, U.S. Air Force Research Laboratory/Air Vehicles Directorate, Wright-Patterson AFB, 1998.
- [21]Menter F R. Two-equation eddy viscosity turbulence models for engineering applications, *AIAA*, Vol. 3, No. 8, pp 1598-1606, 1994
- [22] Frank W. Fluid Mechanics. 7th edition, McGraw, 2009
- [23]Roache P J. Perspective: A method for uniform reporting of grid refinement studies, *J. Fluids Eng.*, Vol. 116, No. 3 pp 405-413
- [24] NASA. Basis for computation of main tables of atmospheric properties. Technical Memorandum, NOAA-S/T-76-1562, NASA-TM-X-74335, 1976